Fluorographene: A Wide Bandgap Semiconductor with Ultraviolet Luminescence

Ki-Joon Jeon,[†,*] Zonghoon Lee,[‡] Elad Pollak,[†] Luca Moreschini,[§] Aaron Bostwick,[§] Cheol-Min Park,[†,⊥] Rueben Mendelsberg,[¶] Velimir Radmilovic,[‡] Robert Kostecki,[†] Thomas J. Richardson,[†] and Eli Rotenberg[§,*]

[†]Environmental Energy Technologies Division, [‡]National Center for Electron Microscopy, and [§]Advanced Light Sources, Lawrence Berkeley National Laboratory, Berkeley, California 94720, United States, [⊥]School of Advanced Materials and System Engineering, Kumoh National Institute of Technology, Gumi, Gyeongbuk 730-701, Korea, and [¶]Material Science Division, Lawrence Berkeley National Laboratory, Berkeley, California 94720, United States

ABSTRACT The manipulation of the bandgap of graphene by various means has stirred great interest for potential applications. Here we show that treatment of graphene with xenon difluoride produces a partially fluorinated graphene (fluorographene) with covalent C—F bonding and local sp^3-carbon hybridization. The material was characterized by Fourier transform infrared spectroscopy, Raman spectroscopy, electron energy loss spectroscopy, photoluminescence spectroscopy, and near edge X-ray absorption spectroscopy. These results confirm the structural features of the fluorographane with a bandgap of 3.8 eV, close to that calculated for fluorinated single layer graphene, $(CF)_n$. The material luminesces broadly in the UV and visible light regions, and has optical properties resembling diamond, with both excitonic and direct optical absorption and emission features. These results suggest the use of fluorographane as a new, readily prepared material for electronic, optoelectronic applications, and energy harvesting applications.

KEYWORDS: fluorographene · ultraviolet luminescence · wide bandgap semiconductor · NEXAFS

Graphene has been studied intensively for its fundamental intrinsic properties and potential applications from graphene-based composite materials to electronics.[1−5] Pristine graphene, however, has no band gap and therefore behaves as a metal.[1−4] Thus, opening the bandgap of graphene is an important goal. There have been attempts to manipulate the electronic properties by confining the physical dimensions of graphene (*i.e.*, graphene nanoribbon (GNR)) and by assembly of exfoliated bilayer graphene on a substrate.[6−10] It is difficult, however, to control the width (*ca.* 10 nm) of GNRs or to synthesize large area Bernal-stacked bilayer graphene. Thus, tuning the electronic properties of single layer graphene, which has been scaled up to 30 in. lateral dimensions[11] *via* a chemical route, is highly desirable.

Altering the electronic properties of graphene by placing foreign species on the surfaces of single layer graphene has also been suggested by theoretical calculations.[12,13] Elias *et al.* have reported the preparation and transport properties of a graphane-like $(CH)_n$ substance,[14] and the electronic structure of graphane was directly characterized.[15] Recently, Nair *et al.* reported synthesis of fluorographene and its insulating properties but the electronic structure of fluorographene has not been directly characterized.[16] Here, we describe the synthesis and characterization of fluorographene, and demonstrate the transformation of the carbon network from sp^2- to sp^3-bonding. In addition, we demonstrate that fluorographene is a wide bandgap semiconductor.

RESULTS AND DISCUSSION

Ab initio calculations of thermodynamic and electronic properties of hydrogenated and fluorinated graphene have been reported.[17,18] In fully fluorinated graphene, $(CF)_n$, fluorine is covalently bonded to sp^3-hybridzed bonds to carbon atoms which are elevated above the plane of the original graphene layer. Fluorine preferentially bonds to the next neighbor carbon atoms on the other side of the sheet (Figure 1a). The calculated formation energy per fluorine atom at 298.15 K and 1 bar is −0.61 eV, compared with −0.14 eV per hydrogen atom for graphane.[17,18] The calculated band gap of $(CF)_n$ is 2.96 eV.[18] Graphite fluoride, CF_x, where x may range from 0.1 to nearly 2, is a well-known material used as a lubricant and in the cathodes of primary lithium batteries. It is made by high temperature (typically >500 °C) fluorination of graphite, and is highly disordered and inhomogeneously fluorinated.[19]

Unsupported, high quality graphene[20] was fluorinated by reaction with xenon difluoride (XeF_2) at 250 °C according to eq 1:

$$2C_n + XeF_2 \rightarrow 2(CF)_n + Xe \qquad (1)$$

The hydrophobic character of fluorographene is demonstrated by dispersion in

*Address correspondence to kjjeon@lbl.gov, erotenberg@lbl.gov.

Received for review September 24, 2010 and accepted December 22, 2010.

Published online January 04, 2011
10.1021/nn1025274

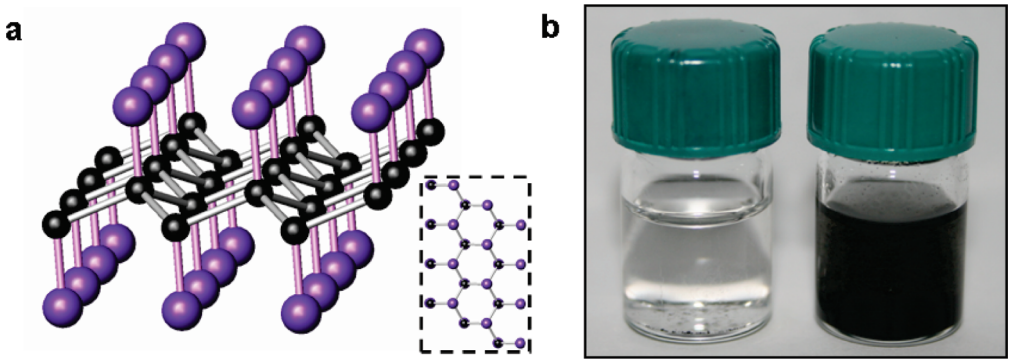

Figure 1. Crystalline structure of fluorographene and the solubility of pristine graphene and fluorographene. (a) Structure of CF; black and purple spheres indicate carbon and fluorine atoms, respectively, which are adsorbed alternatively on both sides of graphene. The inset, dotted area is a plan view. (b) Fluorographene (left vial) and pristine graphene (right vial) in ethanol. These samples were sonicated for 30 s in ethanol.

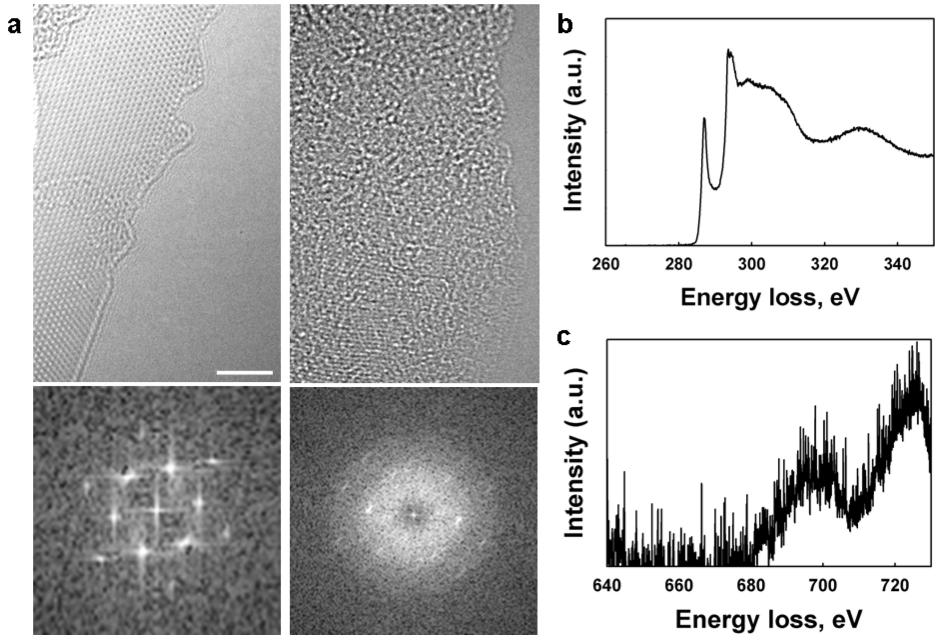

Figure 2. Structural changes of single layer graphene *via* fluorination process: (a) atomic resolution TEM micrographs of single layer graphene and fluorographene at edges and corresponding digital diffractograms; EEL spectra of (b) carbon K-edge (285 eV) and (c) fluorine K-edge (690 eV) corresponding to fluorographene. Scale bar: 2 nm.

ethanol.[21] Pristine graphene (right vial in Figure 1b) is well-dispersed in ethanol because the aromatic ring (*i.e.*, free p_z orbitals; π and π^*) of graphene (sp^2-carbon structure) behaves as an acceptor, forming pseudohydrogen bonds with the ethanol −OH group. On the other hand, fluorographene (left vial in Figure 1b) sinks in ethanol because fluorographene (sp^3-carbon structure) does not have free p_z orbitals to form pseudohydrogen bonds.

In the transmission electron micrographs (Figure 2a), a high-resolution direct imaging of pristine graphene (left image in Figure 2a) shows the hexagonal arrangement of carbon atoms that is characteristic of single layer pristine graphene near the edge.[20] After processing, the fluorographene (right image in Figure 2a) appears to consist of highly fluorinated domains characterized by crumpling and folding of the layer, surrounding planar, graphene-like domains. A digital diffractogram of fluorographene (right diffractogram in Figure 2a) displays the diminished hexagonal diffraction pattern of graphene along with amorphous halos, which is not shown in that of single layer pristine graphene (left diffractogram in Figure 2a). Electron energy loss (EEL) spectra also confirm the presence of fluorine on graphene. It is shown that the carbon K-edge (Figure 2b) is at 285 eV, which is similar to that of graphene, while the fluorine K-edge (Figure 2c) is at 690 eV.

The Fourier transform infrared (FTIR) spectrum of fluorinated graphene obtained in transmission mode (Figure 3a) shows much stronger IR bands in fluorographene than in the graphene due to the greater transparency of the former. Furthermore, a prominent feature at 1260 cm^{-1} characteristic of covalent C−F

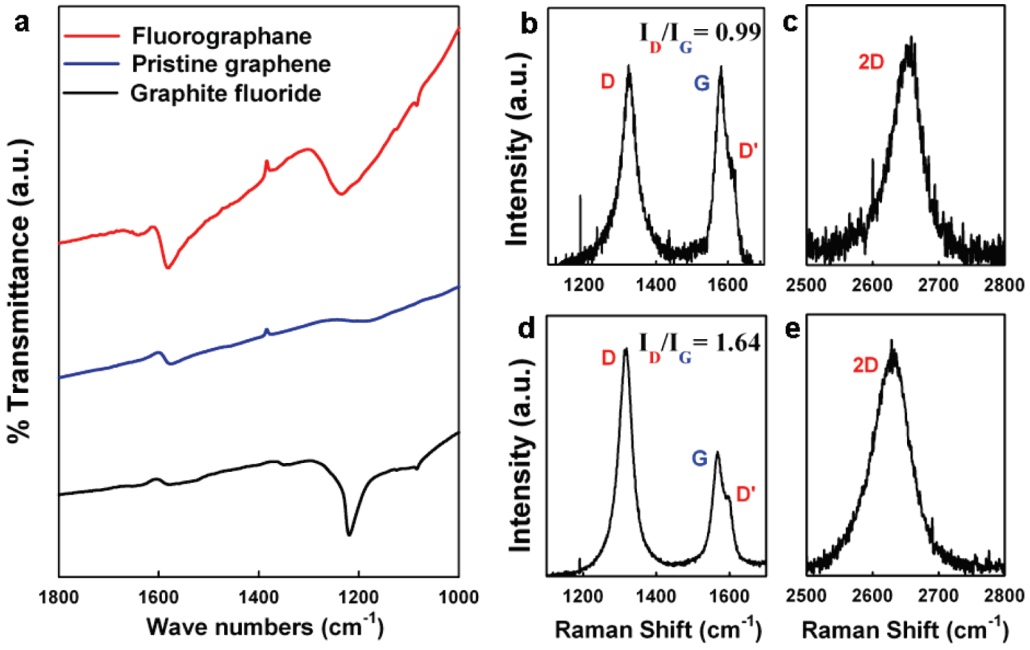

Figure 3. FTIR and Raman spectra of fluorographene and pristine graphene. (a) FTIR spectra of fluorographene, pristine graphene, and graphite fluoride. Micro-Raman spectra of pristine graphene/fluorographene were analyzed and compared. (b) D and G Raman bands of pristine graphene, (c) 2D band of pristine graphene, (d) D and G band of fluorographene, and (e) 2D band of fluorographene.

bond stretching[22] was observed. The spectrum of a commercial sample of graphite fluoride, shown for comparison, has a similar C−F bonding feature. The transparency of the C−F domains also affects the Raman spectrum, which is dominated by the graphene-like domains. The starting material (Figure 3b,c) exhibits the characteristics of single layer graphene with G band at 1580 cm^{-1} and a sharp 2D band at 2670 cm^{-1}.[23,24] After fluorination, the relative intensities of the D and D′ bands have increased (Figure 3d,e). The intensity ratio I_D/I_G (a measure of disorder) changes from 0.99 to 1.64 after fluorination. In addition, a shoulder located at ∼1615 cm^{-1}, denoted as D′, is due to an intravalley process, characteristic of structural disorder in single layer graphene.[24]

The density of states in the few eV above the Fermi level was investigated by near edge X-ray absorption spectroscopy (NEXAFS). Figure 4a shows the NEXAFS spectra at the C 1s threshold acquired at a temperature of 40 K for pristine graphene and fluorographene with two different degrees of fluorination. The pristine graphene spectrum presents the well-known lines at 285.5 and 291.5 eV, corresponding to transitions to the π^* and σ^* conduction states, respectively.[25] That the π^* feature, a characteristic of sp^2 bonding, is progressively decreased with increasing fluorination is direct evidence of the formation of sp^3 bonds in the substance. Two other features gain increasing weight with increasing fluorine content: a clearly defined peak at 287.4 eV and a broader hump at 288.4 eV. We interpret this last feature as the fluorographene conduction band edge. Although its weight is relatively small compared to the main π^* resonance due to an only partial fluorination of the C atoms in the sample, it gives evidence of a substantial shift of the conduction band states in the fluorographene. The peak at 287.4 eV also supports this interpretation: it is much sharper than all other features in the spectrum and we attribute it to an exciton absorption line, reminiscent of the similar scenario present in diamond.[26] From the change in the energy difference between the leading edges of the NEXAFS spectra (dashed lines in Figure 4a) and the corresponding C 1s core level binding energies for pristine graphene and fluorographene we determine a lower limit of 3.8 eV for the fluorographene band gap, close to but larger than the theoretical value, which appears to be a common issue with the generalized gradient approximation.[27] Note however that this sets only a lower limit to the gap value, since the energy of the top of the valence band is ill-defined by our photoemission measurements and it not accessible NEXAFS.

To explore the bandgap opening of fluorographene, we used photoluminescence (PL) spectroscopy which is a reliable, nondestructive optical technique for electronic bandgap measurement.[28] Room temperature PL was carried out on pristine graphene and fluorographene dispersed in acetone using 290 nm (4.275 eV) excitation and a CCD spectrometer. No PL emission was observed in pristine graphene because it has no bandgap.[2,4] However the fluorographene shows two distinct PL peaks at around 3.80 and 3.65 eV, confirming the formation of a wide bandgap semiconductor. The peak at 3.80 eV is at the same energy measured for

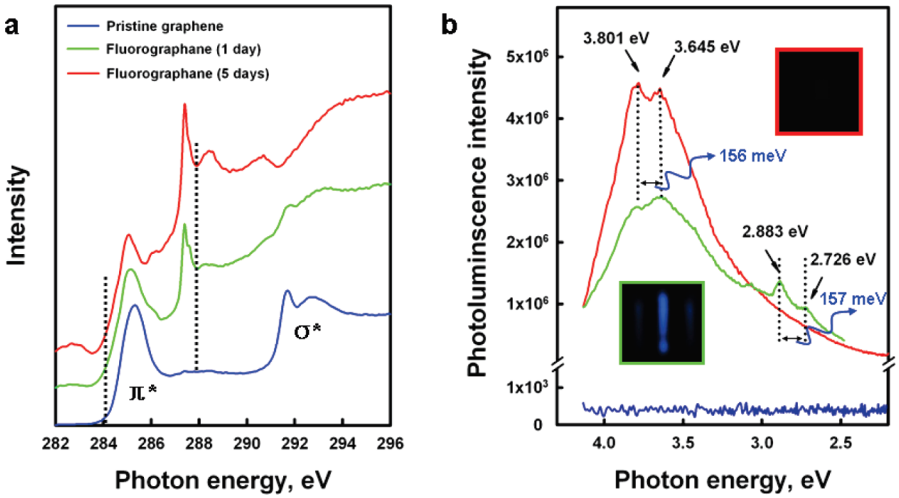

Figure 4. Bandgap opening of fluorographene. (a) NEXAFS spectra of pristine graphene and fluorographene with two different contents of fluorine. The dashed lines at 284.1 and 287.9 eV mark the leading edges of the π^* resonance for the pristine and fluorinated sample, respectively. (b) Room temperature photoluminescence emission of the pristine graphene/fluorographene dispersed in acetone using 290 nm (4.275 eV) excitation. The dotted lines are used for guiding eyes. The interval of dotted line is ~156 meV. Optical images (top view) of the blue emission observed after the PL emission was recorded with the samples in 3.5 mL quartz cuvettes. The blue light persists *ca.* 30 s after the excitation laser is turned off.

the bandgap by NEXFAS. Thus it is attributed to band-to-band recombination of a free electron and a free hole. The 3.645 eV peak is 156 meV (1260 cm^{-1}) below the bandgap emission, equivalent to the C−F vibration mode and consistent with FTIR measurements shown in Figure 3a. As such, this feature is due to phonon-assisted radiative recombination across the bandgap where the C−F vibration mode is excited when the electron−hole pair recombines. Deeper within the gap some blue emission at 2.88 eV was observed in graphene fluorinated for 1 day, as indicated in Figure 4b. It was also accompanied by a second peak located 157 meV lower in energy.

The blue emission is similar to that observed in other luminescent carbon materials,[29,30] the exact origin of which is still controversial. In our case it could be due to excitonic recombination, since the ~1 eV shift of these lines from the peak of the PL emission is similar to the observed excitonic absorption peak seen in the NEXAFS spectrum. However, the blue lines are not robust with increasing fluorination, indicating that excitonic recombination is quenched by the associated morphological changes observed.

In conclusion, we report preparation of fluorographene by direct chemical fluorination of pure graphene. The samples are robust to exposure to air and ethanol. The modification of the carbon−carbon bonding by formation of sp^3-derived carbon−fluorine bonds leads to the formation of a bandgap. The bandgap of fluorographene is at least 3.8 eV, wide enough for optoelectronic applications in the blue/UV spectrum. Fluorographene may pave the way to develop novel graphene-based semiconductors by simple chemical methods for future semiconductor devices and energy harvesting.

MATERIAL AND METHODS

Synthesis Method. The fluorographene sheets were synthesized by heating the mixture of graphene sheets and XeF_2. This mixture was heated to 350 °C for 1 and 5 days under inert atmosphere.

Characterization Methods. *FTIR.* The FT-IR spectrum (400−4000 cm^{-1}) of the pristine graphene and fluorographene was measured using a Nicolet IR100 FT-IR spectrometer with pure KBr as the background. Pristine graphene and fluorographene sheets were mixed with KBr powder and compressed into a transparent tablet for measurements.

TEM and EELS. Transmission electron aberration-corrected microscope (TEAM 0.5, monochromated 80 kV accelerating voltage) were used to perform electron energy loss spectroscopy (EELS) and high-resolution imaging, respectively. Fluorographene sheet was dispersed in acetone. A drop of the suspension was deposited onto commercially available TEM grid (Ted Pella, lacey carbon 300 mesh Cu grids), directly before the TEM session. The contrast for the Figure 2a was adjusted.

Raman Spectroscopy. Raman spectroscopy characterization was also performed. Synthesized samples were placed on a silicon substrate. Raman spectra of fluorographene samples were measured in the back scattering configuration using a micro-Raman spectrometer, (Labram, ISA Groupe Horiba), and holographic grating of 1800 grooves/mm with a He−Ne laser (excitation line 632.8 nm), objective 80× (numerical aperture 0.75). The laser power was reduced to <0.8 mW to avoid sample heating. Peak positions and bandwidths were obtained by fitting with a Lorenztian function.

Near Edge X-ray Absorption Spectroscopy. Data were collected with a Scienta 4000 electrostatic analyzer by measuring the number of photoemitted electrons in the range between 35 and 45 eV kinetic energy, as a function of the incident photon

energy. This is essentially equivalent to the well-known total electron yield mode.

Photoluminescence. PL spectra were recorded on a Jobin Yvon Horiba Fluorolog 3. PL spectra were taken at room temperature. Possible contributions to the PL from the electrical and optical backgrounds along with nonlinearity in the measured wavelengths were eliminated by standard calibration techniques.

Acknowledgment. This work was supported as part of the Northeastern Center for Chemical Energy Storage, an Energy Frontier Research Center funded by the U.S. Department of Energy, Office of Science, Office of Basic Energy Sciences under Award Number DE-SC0001294 and by the National Center for Electron Microscopy, Lawrence Berkeley Lab, which is supported by the US Department of Energy under Contract No. DE-AC02-05CH11231. The Advanced Light Source is supported by the Director, Office of Science, Office of Basic Energy Sciences, of the U.S. Department of Energy under Contract No. DE-AC02-05CH11231. We also thank Dr. Albert Dato and Dr. Michael Frenklach for supplying pristine graphene. L.M. acknowledges support from the Swiss National Science Foundation (SNSF) through Grant PBELP2-125484.

REFERENCES AND NOTES

1. Geim, A. K.; Novoselov, K. S. The Rise of Graphene. *Nat. Mater.* **2007,** *6*, 183–191.
2. Geim, A. K.; Kim, P. Carbon Wonderland. *Sci. Am.* **2008,** *298*, 90–97.
3. Novoselov, K. S.; Geim, A. K.; Morozov, S. V.; Jiang, D.; Katsnelson, M. I.; Grigorieva, I. V.; Dubonos, S. V.; Firsov, A. A. Two-Dimensional Gas of Massless Dirac Fermions in Graphene. *Nature* **2005,** *438*, 197–200.
4. Novoselov, K. S.; Geim, A. K.; Morozov, S. V.; Jiang, D.; Zhang, Y.; Dubonos, S. V.; Grigorieva, I. V.; Firsov, A. A. Electric Field Effect in Atomically Thin Carbon Films. *Science* **2004,** *306*, 666–669.
5. Stankovich, S.; Dikin, D. A.; Dommett, G. H. B.; Kohlhaas, K. M.; Zimney, E. J.; Stach, E. A.; Piner, R. D.; Nguyen, S. T.; Ruoff, R. S. Graphene-Based Composite Materials. *Nature* **2006,** *442*, 282–286.
6. Allen, M. J.; Tung, V. C.; Kaner, R. B. Honeycomb Carbon: A Review of Graphene. *Chem. Rev.* **2009,** *110*, 132–145.
7. Ohta, T.; Bostwick, A.; Seyller, T.; Horn, K.; Rotenberg, E. Controlling the Electronic Structure of Bilayer Graphene. *Science* **2006,** *313*, 951–954.
8. Oostinga, J. B.; Heersche, H. B.; Liu, X.; Morpurgo, A. F.; Vandersypen, L. M. K. Gate-Induced Insulating State in Bilayer Graphene Devices. *Nat. Mater.* **2008,** *7*, 151–157.
9. Zhou, S. Y.; Gweon, G. H.; Fedorov, A. V.; First, P. N.; de Heer, W. A.; Lee, D. H.; Guinea, F.; Castro Neto, A. H.; Lanzara, A. Substrate-Induced Bandgap Opening in Epitaxial Graphene. *Nat. Mater.* **2007,** *6*, 770–775.
10. Zhang, Y.; Tang, T.-T.; Girit, C.; Hao, Z.; Martin, M. C.; Zettl, A.; Crommie, M. F.; Shen, Y. R.; Wang, F. Direct Observation of a Widely Tunable Bandgap in Bilayer Graphene. *Nature* **2009,** *459*, 820–823.
11. Bae, S.; Kim, H.; Lee, Y.; Xu, X.; Park, J.-S.; Zheng, Y.; Balakrishnan, J.; Lei, T.; Ri Kim, H.; Song, Y. I.; *et al.* Roll-to-Roll Production of 30-Inch Graphene Films for Transparent Electrodes. *Nat. Nano* **2010,** *5*, 574–578.
12. Boukhvalov, D. W.; Katsnelson, M. I.; Lichtenstein, A. I. Hydrogen on Graphene: Electronic Structure, Total Energy, Structural Distortions and Magnetism from First-Principles Calculations. *Phys. Rev. B* **2008,** *7*, 035427.
13. Sofo, J. O.; Chaudhari, A. S.; Barber, G. D. Graphane: A Two-Dimensional Hydrocarbon. *Phys. Rev. B* **2007,** *75*, 153401.
14. Elias, D. C.; Nair, R. R.; Mohiuddin, T. M. G.; Morozov, S. V.; Blake, P.; Halsall, M. P.; Ferrari, A. C.; Boukhvalov, D. W.; Katsnelson, M. I.; Geim, A. K.; *et al*. Control of Graphene's Properties by Reversible Hydrogenation: Evidence for Graphane. *Science* **2009,** *323*, 610–613.
15. Haberer, D.; Vyalikh, D. V.; Taioli, S.; Dora, B.; Farjam, M.; Fink, J.; Marchenko, D.; Pichler, T.; Ziegler, K.; Simonucci, S.; *et al.* Tunable Band Gap in Hydrogenated Quasi-free-standing Graphene. *Nano Lett.* **2010,** *10*, 3360.
16. Nair, R. R.; Ren, W.; Jalil, R.; Riaz, I.; Kravets, V. G.; Britnell, L.; Blake, P.; Schedin, F.; Mayorov, A. S.; Yuan, S.; *et al.*, Fluorographene: A Two-Dimensional Counterpart of Teflon. *Small* **2010**, *6*, 2877−2884.
17. Zhou, J.; Wu, M. M.; Zhou, X.; Sun, Q. Tuning Electronic and Magnetic Properties of Graphene by Surface Modification. *Appl. Phys. Lett.* **2009,** *95*, 103108.
18. Zhou, J.; Liang, Q.; Dong, J. Enhanced Spin−Orbit Coupling in Hydrogenated and Fluorinated Graphene. *Carbon* **2010,** *48*, 1405–1409.
19. Watanabe, N. Two Types of Graphite Fluorides, $(CF)_n$ and $(C_2F)_n$, and Discharge Characteristics and Mechanisms of Electrodes of $(CF)_n$ and $(C_2F)_n$ in Lithium Batteries. *Solid State Ionics* **1980,** *1*, 87–110.
20. Dato, A.; Lee, Z.; Jeon, K. J.; Erni, R.; Radmilovic, V.; Richardson, T. J.; Frenklach, M. Clean and Highly Ordered Graphene Synthesized in the Gas Phase. *Chem. Commun.* **2009,** 6095–6097.
21. Levitt, M.; Perutz, M. F. Aromatic Rings Act as Hydrogen-Bond Acceptors. *J. Mol. Biol.* **1988,** *201*, 751–754.
22. Bon, S. B.; Valentini, L.; Verdejo, R.; Garcia Fierro, J. L.; Peponi, L.; Lopez-Manchado, M. A.; Kenny, J. M. Plasma Fluorination of Chemically Derived Graphene Sheets and Subsequent Modification with Butylamine. *Chem. Mater.* **2009,** *21*, 3433–3438.
23. Ferrari, A. C.; Meyer, J. C.; Scardaci, V.; Casiraghi, C.; Lazzeri, M.; Mauri, F.; Piscanec, S.; Jiang, D.; Novoselov, K. S.; Roth, S.; *et al*. Raman Spectrum of Graphene and Graphene Layers. *Phys. Rev. Lett.* **2006,** *97*, 187401.
24. Ferrari, A. C. Raman Spectroscopy of Graphene and Graphite: Disorder, Electron-Phonon Coupling, Doping and Nonadiabatic Effects. *Solid State Commun.* **2007,** *143*, 47–57.
25. Pacile, D.; Papagno, M.; Rodriguez, A. F.; Grioni, M.; Papagno, L.; Girit, C. O.; Meyer, J. C.; Begtrup, G. E.; Zettl, A. Near-Edge X-Ray Absorption Fine-Structure Investigation of Graphene. *Phys. Rev. Lett.* **2008,** *101*, 066806.
26. Coffman, F. L.; Cao, R.; Pianetta, P. A.; Kapoor, S.; Kelly, M.; Terminello, L. J. Near-Edge X-Ray Absorption of Carbon Materials for Determining Bond Hybridization in Mixed sp^2/sp^3 Bonded Materials. *Appl. Phys. Lett.* **1996,** *69*, 568.
27. Klintenberg, M.; Levegue, S.; Katsnelson, M. I.; Eriksson, O. Theoretical Analysis of the Chemical Bonding and Electronic Structure of Graphene Interacting with Group IA and Group VIIA Elements. *Phys. Rev. B* **2010,** *81*, 085433.
28. Wang, J.; Gudiksen, M. S.; Duan, X.; Cui, Y.; Lieber, C. M. Highly Polarized Photoluminescence and Photodetection from Single Indium Phosphide Nanowires. *Science* **2001,** *293*, 1455–1457.
29. Dengyu, P.; Jingchun, Z.; Zhen, L.; Minghong, W., Hydrothermal Route for Cutting Graphene Sheets into Blue-Luminescent Graphene Quantum Dots. *Adv. Mater. 22*, 734-738.
30. Goki, E.; Yun-Yue, L.; Cecilia, M.; Hisato, Y.; Hsin-An, C.; Chen, I. S.; Chun-Wei, C.; Manish, C. Blue Photoluminescence from Chemically Derived Graphene Oxide. *Adv. Mater.* **2010,** *22*, 505–509.